RNA-Seq and Network Analysis Reveal Unique Chemokine Activity Gene Expression Signatures in Synovial Tissue From Rheumatoid Arthritis

Runrun Zhang
Shanghai University of Traditional Chinese Medicine
Yehua Jin
Shanghai University of Traditional Chinese Medicine
Cen Chang
Shanghai University of Traditional Chinese Medicine
Xinpeng Zhou
Shandong University of Traditional Chinese Medicine Affiliated Hospital
Yanqin Bian
Guanghua Hospital: Shanghai Guanghua Hospital of Integrated Traditional Chinese and Western Medicine
Yu Shen
Guanghua Hospital: Shanghai Guanghua Hospital of Integrated Traditional Chinese and Western Medicine
Yang Sun
Guanghua Hospital: Shanghai Guanghua Hospital of Integrated Traditional Chinese and Western Medicine
Steven J. Schrodi
University of Wisconsin-Madison
Songtao Sun (sstever0156258@aliyun.com)
Guanghua Hospital: Shanghai Guanghua Hospital of Integrated Traditional Chinese and Western Medicine
Shicheng Guo
University of Wisconsin-Madison
dongyi He
Guanghua Hospital: Shanghai Guanghua Hospital of Integrated Traditional Chinese and Western Medicine

---

Research article

Keywords: Rheumatoid Arthritis, Osteoarthritis, Synovial Tissue, Gene Expression, RNA-Seq

Posted Date: May 13th, 2021

DOI: https://doi.org/10.21203/rs.3.rs-510087/v1

Abstract

Objective: This study identified to provide a comprehensive understanding of genome-wide expression patterns of synovial tissue from rheumatoid arthritis (RA) patients to investigate the potential mechanism RA occurrence and development.

Methods: The transcription profiles of 9 RA and 15 control (osteoarthritis OA) synovial tissue were generated by RNA-Seq. Gene set enrichment analysis (GSEA) was used to analyze all detected genes and differentially expressed genes (DEGs) were identified by DESeq. To further analyze the DEGs, Gene ontology (GO) functional enrichment and Kyoto Encyclopedia of Genes and Genomes (KEGG) pathway analysis were performed. The protein-protein interaction (PPI) network of DEGs were constructed by STRING and the hub genes were identified by topology clustering with MCODE-Cytoscape. The most important hub genes were validated by quantitative real time polymerase chain reaction (qRT-PCR).

Results: A total of 17736 genes were detected and 651 DEGs were identified. For the GSEA, significantly enriched gene sets positively correlated with the RA group were CD40 signaling over-activation, Th1 cytotoxic module in C2, over-activation of immune response, adaptive immune response in C5, In C7, the up-regulation of the gene set of effective versus memory CD8 T cell is related to RA group. The down-regulation of gene set of naïve versus effective CD8 T cell is related to RA group.in C7. Biology process enrichment analysis showed that the DEGs were significantly enriched for signal transduction ($P=1.52\times10^{-08}$), immune response ($P=1.94\times10^{-22}$) and inflammatory response ($P=1.11\times10^{-11}$). Molecule function enrichment analysis revealed over-represented calcium ion binding ($P=8.61\times10^{-03}$), receptor binding ($P=7.03\times10^{-05}$) and chemokine activity ($P=4.15\times10^{-15}$). The DEGs were significantly enriched for plasma membrane ($P=2.26\times10^{-20}$), integral component of membrane ($P=7.79\times10^{-07}$), extracellular region ($P=3.43\times10^{-16}$) in cellular component. The KEGG pathway analysis showed that the DEGs were enriched in the cytokine-cytokine receptor interaction ($P=6.86\times10^{-21}$), chemokine signaling pathway ($P=2.03\times10^{-11}$), systemic lupus erythematosus($P=9.23\times10^{-07}$), T cell receptor signaling pathway ($P=6.59\times10^{-06}$) and rheumatoid arthritis ($P=3.24\times10^{-05}$). We confirmed RA over-expressed PPI network hub genes included *CXCL13*, *CXCL6*, *CCR5*, *CXCR5*, *CCR2*, *CXCL3*, *CXCL10* and RA down-regulated hub genes included *SSTR1*.

Conclusions: The study identified and verified the DEGs between RA and OA synovial tissue which highlighted the activity of a subset of chemokine genes, thereby providing novel insights into the molecular mechanisms of RA pathogenesis and identified potential diagnostic and therapeutic targets for RA.

1. Introduction

Rheumatoid arthritis (RA) is an autoimmune diseases characterized by synovial inflammation and hyperplasia, cartilage and bone destruction, and the clinical manifestations are joint pain, swelling, stiffness, and deformation [1, 2]. The pathogenesis of RA is thought to involve genetics, environment

factors, obesity, diet, and microbiota [3]. Osteoarthritis (OA) is a joint disease characterized by degeneration of synovial joint and loss of articular cartilage, with the primary clinical features including pain and loss of mobility [4]. Genetics, diet, estrogen use, obesity, bone density, and joint laxity all play a role in OA [5]. As both RA and OA share common physiological targets, the exploration of synovial tissue biomarkers that discriminate between these diseases carries substantial medical utility [6, 7].

Transcriptomics is tissue-specific and as such offers an avenue for the investigation of effects localized to cells that are likely to play an important role to the etiology of diseases [8]. RNA sequencing (RNA-Seq) technology has become a primary took of transcriptomics research to characterize expression within certain cell types and tissues. Using RNA-seq to identify gene expression differences between RA and OA synovial tissue may provide new insights into the understanding of the molecular pathophysiology of these diseases.

In this study, to better understand the transcriptome functional differences between RA and OA, we analyzed whole detected genes by GSEA, identified the differentially expressed genes (DEGs) between RA and OA synovial tissue using RNA-seq, then analyzed the DEGs by Gene ontology (GO) functional enrichment and Kyoto Encyclopedia of Genes and Genomes (KEGG) pathway analysis, constructed protein-protein interaction (PPI) network, screened and verified the hub genes. Due to their central role in gene expression networks, validated hub genes may serve as critically important molecular markers for identifying RA and OA differences in synovial tissue.

2. Material And Methods

2.1 Patients/Tissue

This study included 9 RA patients, who were diagnosed based on the 2010 American College of Rheumatology (ACR)/European League Against Rheumatism (EULAR) classification criteria for rheumatoid arthritis[9], 15 OA patients, who were diagnosed on the American College of Rheumatology OA classification criteria [10]. The synovial tissue of RA and OA patients were obtained from Guanghua hospital, Shanghai. After taking the synovial tissue, removed the excess fat and vascular tissue, and then put them into liquid nitrogen for later use. The demographic information was shown in **Supplementary Table1**.This study was approved by the Ethics Committee of Guanghua Hospital of Integrated Traditional Chinese and Western Medicine (approval number: 2018-K-12) and written consent was collected prior to the surgery from the patients.

2.2 Ribonucleic acid isolation and Library Preparation

Total ribonucleic acid (RNA) from the synovial tissue was extracted using the Trizol reagent (Thermo Fisher, Waltham, MA, USA) according to the manufacturer's protocol. RNA purity and quantification were evaluated using the Nano Drop 2000 spectrophotometer (Thermo Scientific, Wilmington, DE, USA). RNA integrity was assessed using the Agilent 2100 Bioanalyzer (Agilent Technologies, Santa Clara, CA, USA).

The total RNA that had a standard of RNA integrity number (RIN)≥7.0, 28S/18S≥0.7 was subjected to RNA-Seq. Then the libraries were constructed using TruSeq Stranded mRNA LT Sample Prep Kit (Illumina, San Diego, CA, USA) according to the manufacturer's instructions.

2.3 RNA Sequencing and Differentially Expressed Genes Identification

The libraries were sequenced on an Illumina HiSeq X Ten platform. Raw data (raw reads) of fastq format were firstly processed using Trimmomatic [11] and the low quality reads were removed to obtain the clean reads. The clean reads were mapped to the human genome (GRCh38) using HISAT2[12]. FPKM of each gene was calculated using Cufflinks[14,15], and the read counts of each gene were obtained by HTSeqcount[15]. Differential expression analysis was performed using the DESeq R package[16]. P value < 0.05 and |log2FoldChange| >= 2 were set as the threshold for significant differential expression.

2.4 The Gene Set Enrichment Analysis of All Detected Genes

Gene set enrichment analysis (GSEA) is used to determine the statistically significant differences between two groups with regard to a defined set of genes. The analysis was conducted using the R software package, and the data set was from the Molecular Signatures Database v7.2 (MSigDB)downloaded from the *GSEA-MSigDB* websites.The MSigDB is database of gene sets for performing gene set enrichment analysis[17]. Adjusted P-value < 0.05, |NES| >1, P<0.05, FDR<0.25 were selected as the cut-off criteria indicating statistically significant differences. The MSigDB gene sets included 9 major collections (H:C8). C2 (curated gene sets), C5 (ontology gene sets), C7 (immunologic signature gene sets) are the target data set for our study.

2.5 The GO functional enrichment and KEGG pathway analysis

The DEGs were annotated by the GO functional enrichment analysis which included biological process (BP), molecular function (MF), cellular component (CC) and KEGG pathway analysis[18]. KEGG is a database resource for elucidating the genes function at the molecular and higher levels, including biochemical pathways[19]. The annotation and visualization were performed by the clusterProfiler package[20] (an R package for comparing biological themes among gene clusters). The enrichment analysis was performed by hypergeometric test. P<0.05 was chosen as the cut-off criterion indicating statistically significant difference.

2.6 The PPI network construction and hub genes identification

The PPI network was constructed by the Search Tool for the Retrieval of Interacting Genes/Proteins (STRING), a database providing all the exposed protein-protein interactions[21]. The setting of minimum required interaction score was highest confidence (0.900). The hub genes were screened and visualized by the MCODE and CytoHubba plugins in Cytoscape version 3.7.2. The Cytoscape software can visualize, model and analyze molecular and genetic interaction networks[22]. MCODE and cytoHubba plugins can identify hub genes from complex interaction and help to lock the hub-genes in a computationally efficient manner [23].

2.7 Validation of hub gene expression by reverse transcription polymerase chain reaction

The reverse transcription polymerase chain reaction (qRT-PCR) was conducted to validate the reliability of the DEG results, the expression levels of 10 selected hub genes were determined. Total RNA were extracted from the 9 RA and 15 OA synovial tissue with TRIzol reagent (Invitrogen, Thermo Fisher Scientific, Inc). The RNA samples were reverse transcribed to cDNA with PrimeScript™ RT Master Mix (Perfect Real Time) (Takara, China), and qRT-PCR was carried out using TB Green® Premix Ex Taq™ (Tli RNaseH Plus) (Takara, China). β-actin was used as an internal reference. Relative mRNA expression was calculated using the $2^{-\Delta\Delta}$Ct method. Mann Whitney test was used for the statistical analysis, and $P < 0.05$ indicated a significant difference.

3. Results

3.1 The Total Detected Genes and Differentially Expressed Genes Identification

In our sequencing data, a total of 17,736 genes were detected and 651 differential expression genes were identified with the threshold of P value < 0.05 and |log2FoldChange| ≥ 2. We identified 403 up-regulated and 248 down-regulated differential expressed genes. The volcano plot of DEGs were shown in Fig. 1.

3.2 The GSEA of Total Detected Genes

The GSEA was performed to identify differentially expressed gene sets between RA and OA group. In C3 (curated gene sets), the significant enriched gene sets positively correlated with RA group were CD40 signaling up (NES = 2.38, P < 0.0001, FDR = 6.16×10^{-9}), Th1 cytotoxic module (NES = 2.50, P < 0.0001, FDR = 6.16×10^{-9}) (Fig. 2A). In C5 (ontology gene sets), the significant enriched gene sets positively correlated with RA group were activation of immune response (NES = 2.15, P < 0.0001, FDR = 1.23×10^{-9}), adaptive immune response (NES = 2.62, P < 0.0001, FDR = 1.23×10^{-9}) (Fig. 2B). In C7, the up-regulation of

the gene set of effective versus memory CD8 T cell is related to RA-related genes (NES = 2.13, P < 0.0001, FDR = 3.17×10^{-9}). The down-regulation of gene set of naïve versus effective CD8 T cell is related to RA-related genes (NES = 2.39, P < 0.0001, FDR = 3.17×10^{-9}) (Fig. 2C).

3.3 The GO functional enrichment and KEGG pathway analysis of DEGs

The results of GO functional enrichment analysis showed that the DEGs were enriched in signal transduction, immune response and inflammatory response for BP, the DEGs were enriched in calcium ion binding, receptor binding and chemokine activity for MF, and the DEGs were enriched in plasma membrane, integral component of membrane and extracellular region for CC (Fig. 3A, 3B). The KEGG pathway analysis showed that the DEGs were enriched in the cytokine-cytokine receptor interaction, chemokine signaling pathway, systemic lupus erythematosus, T cell receptor signaling pathway and rheumatoid arthritis (Fig. 3C, 3D). The important pathway of cytokine-cytokine receptor interaction and rheumatoid arthritis was shown in Fig. 4.

3.4 The PPI network construction and hub genes identification

Using the STRING database, our analysis produced a total 630 nodes and 1001 edges. The PPI enrichment p-value was 1.0×10^{-16}. Through MCODE plugin in Cytoscape software, 19 modules were identified. The top 5 modules were shown in Fig. 5. Combined with MCODE and cytoHubba plugin in Cytoscape, the hub genes of *CXCL13, CXCL6, CCR5, CXCR5, CCR2, CXCL3, CXCL10, CCR7, SSTR1, SSTR3* were identified for further analysis.

3.5 Validation of hub gene expression by qRT-PCR

Try to verified the hub genes, the expression levels of 10 selected hub genes in RA and OA synovial tissue were detected by the qRT-PCR. The primer sequence was shown in Table 3. The statistical results showed that the expression levels of *CXCL13*(P < 0.0001), *CXCL6* (P = 0.0252), *CCR5* (P = 0.0002), *CXCR5* (P = 0.0033), *CCR2* (P = 0.0073), *CXCL3* (P = 0.0314), *CXCL10* (P < 0.0001) in RA synovial tissue were higher than that in OA synovial tissue and the expression levels of *SSTR1* (P = 0.0486) in OA synovial tissue were higher than that in RA synovial tissue (Fig. 6).

4. Discussion

RA and OA are two common types of arthritis with an inflammatory component, but have distinct etiologies, clinical trajectories and treatment. The pathogenesis and manifestations of these two diseases are complex, with clinical heterogeneity in presentation and disease course. Distinguishing between these two arthritic conditions is critically important for early diagnosis, appropriate treatment and elucidates the underlying pathophysiology of these disorders. Studies have demonstrated that synovial tissue plays an important role in the occurrence and development of both RA and OA. Our study

performed second-generation sequencing on the synovial tissue of these two diseases, thereby enabling the identification of DEGs, analysis of the functions and pathways from DEGs enrichment results, and subsequently verified the hub DEGs by RT-qPCR.

In previous studies, the data sets in the GEO database were used for bioinformatics analysis of RA synovial tissue, such as GSE55235, GSE12021, etc. These studies are based on previous chip information, with different data sets and different genes identified[24, 25]. To further investigate the biomarkers of synovial tissue in RA synovial tissue. In order to further analyze the transcriptome of RA synovial tissue derived from patients in a clinical setting, we collected synovial tissue from patients with RA and OA within a single rheumatology hospital, performed RNA-seq, and investigated the pathways, gene networks and hub genes to further arthritis transcriptome studies.

In this study, a total of 17736 genes were detected. The GSEA was sensitive to detect genes with relatively smaller fold change [26]. We found that in curated gene sets, the significant enriched gene sets positively correlated with RA group were CD40 signaling up, Th1 cytotoxic module. The CD40 signaling is associated with the production of human rheumatoid factor [27] and the CD40/NF-kB signaling pathway play an important role in RA pathogenesis[28].The Th1 cytotoxic module has not been reported to be related to RA, but the Th1 cytotoxic is reportedly associated with tumor microenvironment[29]. In ontology gene sets, the significant enriched gene sets positively correlated with RA group were activation of immune response, adaptive immune response. The RA is an autoimmune disease involved in innate and adaptive immunity[30]. In immunologic signature gene sets, the significant enriched gene sets positively correlated with RA group was the up-regulation of the gene set of effective versus memory CD8 T cell; The down-regulation of gene set of naïve versus effective CD8 T cell.

-The CD8 + T cells are involved in the pathogenesis of many autoimmune diseases mainly due to their self-reactive cytotoxic inflammatory behavior[31]. Effective CD8 + T cells have proliferation and cytotoxic properties, and induce the death of infected cells and effective memory CD8 + T cells have a lower ability to induce cytotoxicity than effective CD8 + T cells[31, 32].

In our study, a total of 651 DEGs were identified, of which 403 were up-regulated genes and 248 were down-regulated genes. GO functional enrichment analysis demonstrated that the DEGs were enriched in signal transduction, immune response and inflammatory response in BP term, enriched in calcium ion binding, receptor binding and chemokine activity in MF term, enriched in plasma membrane, integral component of membrane and extracellular region in CC term. The KEGG pathway analysis showed that the DEGs were enriched in the cytokine-cytokine receptor interaction, chemokine signaling pathway, systemic lupus erythematosus, T cell receptor signaling pathway and rheumatoid arthritis. The DEGs was mainly concentrated in immune and inflammation-related pathways.

A total of 10 DEGs were distinguished as hub genes by MCODE and cytoHubba plugin of Cytoscape. According to the ROC analysis, and qRT-PCR validation, for the synovial tissue ,the expression of *CXCL13, CXCL6, CCR5, CXCR5, CCR2, CXCL3, CXCL10* in RA were higher than OA,but the expression of *SSTR1* in OA was higher than RA. The expression of CCR7 and SSTR3 showed no difference between RA and OA

synovial tissue. *CXCL13, CXCL10, CXCL6 and CXCL3* are the main members of the CXC chemokine subfamily. C-X-C motif chemokine ligand 13 (CXCL13), a B cell chemokine, interacting with its receptor C-X-C motif chemokine receptor 5 (*CXCR5*) promotes the migration and aggregation of B lymphocytes [33]. The expression level of *CXCL13* with the serum of RA patients are positively correlated with the level of rheumatoid factor, and is also correlated with the disease activity and treatment response of early rheumatoid arthritis [34–36]. C-X-C motif chemokine ligand 10 (*CXCL10*) is a ligand for the receptor C-X-C motif chemokine receptor 3 (*CXCR3*), which may stimulate the migration of monocytes, natural killer and T-cell migration [37]. The expression of *CXCL10* was detected in serum, synovial fluid and synovial tissue of RA patients [38, 39]. *CXCL10* may be a disease activity marker in early RA because of its high circulating level in plasma of untreated early RA and its association with clinical disease activity[40]. Our study confirmed the high expression of *CXCL10* in RA synovial tissue, and identified that *CXCL10* expression level in RA synovial tissue was higher than that in OA synovial tissue, and the difference was statistically significant. C-X-C motif chemokine ligand 3 (*CXCL3*) was reported to be associated with the invasion and metastasis of various cancer[41–43]. CXCL3 and CXCL6 are related to the invasion and migration of a variety of cancers [44–46]. The differential expression of *CXCL3* and *CXCL6* between RA and OA synovial tissue has not been reported. CCR7, CCR5, CCR2 are typical chemokine receptors. C-C motif chemokine receptor 5 (CCR5) is reportedly expressed in the RA synovial tissue and T helper-cell type 1 inflammatory infiltrates. The *CCR5* (the Delta32 allelic variant) has previously been reported as having a protective effect on RA susceptibility [47], however, the effect of CCR5 inhibitors on RA is still controversial[48–50]. C-C motif chemokine receptor 2 (*CCR2*) has been widely considered as a potential therapeutic target for RA and the CCR2 blocking agents have been developed[51]. The monocyte chemoattractantprotein (MCP)-1 (*CCL2*) and its high-affinity receptor, CCR2, are central to the development of pain associated with knee osteoarthritis. *CCR2* plays an important role in both RA and OA. our study found the expression of *CCR2* in RA and OA synovial tissue was different, may further identify its differential function between RA and OA. Somatostatins can regulate diverse cellular functions such as neurotransmission, cell proliferation. The somatostatin receptor 1 (*SSTR1*) was reportedly associated with various cancer, such as prostate cancer[52] and gastric cancer [53]. The role of *SSTR1* in RA and OA has not been studied, our study may provide a basis for future arthritis research.

5. Conclusion

the RNA-seq was used to detect the genes between RA and OA synovial tissue. Combined with bioinformatics analysis, the DEGs were identified and the GO functional and KEGG pathway enrichment analysis of DEGs was analyzed. The hub DEGs, *SSTR1, CXCR5, CXCL6, CXCL3, CXCL13, CXCL10, CCR7, CCR2* were verified by qRT-PCR. The present study could enrich expression profile data of DEGs between RA and OA synovial tissue and provide novel insight into difference between RA and OA. The candidate DEGs, pathway might be therapeutic targets and biomarkers for RA or OA.

Declarations

Acknowledgements

We thank all participating subjects for their kind cooperation in this study.

Authors’ contributions

Dongyi He, Shicheng Guo, Songtao Sun contributed to the conception, design and final approval of the submitted version. Cen Chang, Xinpeng Zhou, Yanqin Bian contributed to the analysis of sequencing data, statistical analysis. Yu Shen, Yang Sun, Songtao Sun collected samples and helped statistic and draft the manuscript. The final manuscript was completed by Runrun Zhang, Yehua Jin. All authors read and approved the final manuscript.

Competing interests

No potential conflicts of interest was disclosed for all the authors.

Ethics approval

This study was approved by the Ethics Committee of Guanghua Hospital of Integrated Traditional Chinese and Western Medicine (approval number: 2018-K-12) and written consent was collected prior to the surgery from the patients.

Funding

This work was funded by the National Natural Science Funds of China (81774114, 82074234), Shanghai Chinese Medicine Development Office, Shanghai Chinese and Western Medicine Clinical Pilot Project (ZY(2018–2020)-FWTX-1010), Shanghai Chinese Medicine Development Office, Shanghai Traditional Chinese Medicine Specialty Alliance Project (ZY(2018-2020)-FWTX-4017), National Administration of Traditional Chinese Medicine, Regional Chinese Medicine (Specialist) Diagnosis and Treatment Center Construction Project-Rheumatology.

Availability of data and materials

The datasets used and/or analyzed during the current study are available from the corresponding author on reasonable request.

Footnotes

Publisher's Note

Springer Nature remains neutral with regard to jurisdictional claims in published maps and institutional affiliations.

Runrun Zhang and Yehua Jin contributed equally to this work.

Contributor Information

Runrun Zhang, Email: runrun0971569@163.com

Yehua Jin, Email: jinyehua1991@163.com

Cen Chang, Email: changcen0928@163.com

Xinpeng Zhou, Email: zhouxinpeng.no.1@163.com

Yanqin Bian, Email: xiaobian504@126.com

Yu Shen, Email: 403084044@qq.com

Yang Sun, Email: shmzx_sy@aliyun.com

Songtao Sun, Email: sstever0156258@aliyun.com

Steven J. Schrodi, Email:schrodi@wisc.edu

Shicheng Guo, Email:shicheng.guo@wisc.edu

Dongyi He, Email: hedongyi1967@shutcm.edu.cn

References

1. McInnes IB. The Pathogenesis of Rheumatoid Arthritis. N Engl J Med. 2011;15.
2. Harnden K, Pease C, Jackson A. Rheumatoid arthritis. BMJ. 2016;i387.
3. Croia C, Bursi R, Sutera D, Petrelli F, Alunno A, Puxeddu I. Review One year in review 2019: pathogenesis of rheumatoid arthritis. Clin Exp Rheumatol. 2019;11.
4. Buckwalter J, Martin J. Osteoarthritis. Adv Drug Deliv Rev. 2006;58:150–67.
5. Felson DT. Osteoarthritis. New Insights. Part 1: The Disease and Its Risk Factors. Ann Intern Med. 2000;133:635.
6. Scott DL, Wolfe F, Huizinga TW. Rheumatoid arthritis. 2010;376:15.
7. Glyn-Jones S, Palmer AJR, Agricola R, Price AJ, Vincent TL, Weinans H, et al. Osteoarthritis The Lancet. 2015;386:376–87.

8. Song X, Lin Q. Genomics, transcriptomics and proteomics to elucidate the pathogenesis of rheumatoid arthritis. Rheumatol Int. 2017;37:1257–65.
9. Aletaha D, Neogi T, Silman AJ, Funovits J, Felson DT, Bingham CO, et al. 2010 Rheumatoid arthritis classification criteria: an American College of Rheumatology/European League Against Rheumatism collaborative initiative. Ann Rheum Dis. 2010;69:1580–8.
10. Altman R, Asch E, Bloch D, Bole G, Borenstein D, Brandt K, et al. Development of criteria for the classification and reporting of osteoarthritis: Classification of osteoarthritis of the knee. Arthritis Rheum. 1986;29:1039–49.
11. Bolger AM, Lohse M, Usadel B. Trimmomatic: a flexible trimmer for Illumina sequence data. Bioinformatics. 2014;30:2114–20.
12. Kim D, Langmead B, Salzberg SL. HISAT: a fast spliced aligner with low memory requirements. Nat Methods. 2015;12:357–60.
13. Roberts A, Trapnell C, Donaghey J, Rinn JL, Pachter L. Improving RNA-Seq expression estimates by correcting for fragment bias. Genome Biol. 2011;12:R22.
14. Trapnell C, Williams BA, Pertea G, Mortazavi A, Kwan G, van Baren MJ, et al. Transcript assembly and quantification by RNA-Seq reveals unannotated transcripts and isoform switching during cell differentiation. Nat Biotechnol. 2010;28:511–5.
15. Anders S, Pyl PT, Huber W. HTSeq – A Python framework to work with high-throughput sequencing data. Bioinformatics. 2015;31:166–9.
16. Simon Anders WH. Differential expression of RNA-Seq data at the gene level – the DESeq package. EMBL. 2012;24.
17. Liberzon A, Birger C, Thorvaldsdóttir H, Ghandi M, Tamayo P. The Molecular Signatures Database (MSigDB) hallmark gene set collection. 2016;18.
18. Ashburner M, Ball CA, Blake JA, Botstein D, Butler H, Cherry JM, et al. Gene Ontology: tool for the unification of biology. Nat Genet. 2000;25:25–9.
19. Kanehisa M, Furumichi M, Tanabe M, Sato Y, Morishima K. KEGG: new perspectives on genomes, pathways, diseases and drugs. Nucleic Acids Res. 2017;45:D353–61.
20. Yu G, Wang L-G, Han Y, He Q-Y. clusterProfiler: an R Package for Comparing Biological Themes Among Gene Clusters. OMICS J Integr Biol. 2012;16:284–7.
21. Szklarczyk D, Gable AL, Lyon D, Junge A, Wyder S, Huerta-Cepas J, et al. STRING v11: protein–protein association networks with increased coverage, supporting functional discovery in genome-wide experimental datasets. Nucleic Acids Res. 2019;47:D607–13.
22. Shannon P. Cytoscape. A Software Environment for Integrated Models of Biomolecular Interaction Networks. Genome Res. 2003;13:2498–504.
23. Chin C-H, Chen S-H, Wu H-H, Ho C-W, Ko M-T, Lin C-Y. cytoHubba: identifying hub objects and sub-networks from complex interactome. BMC Syst Biol. 2014;8:11.

24. Li Z, Xu M, Li R, Zhu Z, Liu Y, Du Z, et al. Identification of biomarkers associated with synovitis in rheumatoid arthritis by bioinformatics analyses. Biosci Rep. 2020;40:BSR20201713.
25. Ren C, Li M, Du W, Lü J, Zheng Y, Xu H, et al. Comprehensive Bioinformatics Analysis Reveals Hub Genes and Inflammation State of Rheumatoid Arthritis. BioMed Res Int. 2020;2020:1–13.
26. Zeng M, Liu J, Yang W, Zhang S, Liu F, Dong Z, et al. Multiple-microarray analysis for identification of hub genes involved in tubulointerstial injury in diabetic nephropathy. J Cell Physiol. 2019;234:16447–62.
27. Kyburz D, Corr M, Brinson DC, Von Damm A, Tighe H, Carson DA. Human rheumatoid factor production is dependent on CD40 signaling and autoantigen. J Immunol Baltim Md 1950 United States. 1999;163:3116–22.
28. Criswell LA. Gene discovery in rheumatoid arthritis highlights the CD^{40}/ NF-jB signaling pathway in disease pathogenesis. Immunol Rev. 2009;7.
29. Tosolini M, Kirilovsky A, Mlecnik B, Fredriksen T, Mauger S, Bindea G, et al. Clinical Impact of Different Classes of Infiltrating T Cytotoxic and Helper Cells (Th1, Th2, Treg, Th17) in Patients with Colorectal Cancer. Cancer Res. 2011;71:1263–71.
30. O'Neil LJ, Kaplan MJ. Neutrophils in Rheumatoid Arthritis: Breaking Immune Tolerance and Fueling Disease. Trends Mol Med. 2019;25:215–27.
31. Carvalheiro H, da Silva JAP, Souto-Carneiro MM. Potential roles for CD8 + T cells in rheumatoid arthritis. Autoimmun Rev. 2013;12:401–9.
32. Tomiyama H, Matsuda T, Takiguchi M. Differentiation of Human CD8 $^{+}$ T Cells from a Memory to Memory/Effector Phenotype. J Immunol. 2002;168:5538–50.
33. Bao Y-Q, Wang J-P, Dai Z-W, Mao Y-M, Wu J, Guo H-S, et al. Increased circulating CXCL13 levels in systemic lupus erythematosus and rheumatoid arthritis: a meta-analysis. Clin Rheumatol. 2020;39:281–90.
34. Greisen SR, Schelde KK, Rasmussen TK, Kragstrup TW, Stengaard-Pedersen K, Hetland ML, et al. CXCL13 predicts disease activity in early rheumatoid arthritis and could be an indicator of the therapeutic `window of opportunity'. Arthritis Res Ther. 2014;16:434.
35. Jones JD, Hamilton B, Challener GJ, de Brum-Fernandes AJ, Cossette P, Liang P, et al. Serum C-X-C motif chemokine 13 is elevated in early and established rheumatoid arthritis and correlates with rheumatoid factor levels. Arthritis Res Ther. 2014;16:R103.
36. Allam SI, Sallam RA, Elghannam DM, El-Ghaweet AI. Clinical significance of serum B cell chemokine (CXCL13) in early rheumatoid arthritis patients. Egypt Rheumatol. 2019;41:11–4.
37. Karin N, Razon H. Chemokines beyond chemo-attraction: CXCL10 and its significant role in cancer and autoimmunity. Cytokine. 2018;109:24–8.
38. Patel DD, Zachariah JP, Whichard LP. CXCR3 and CCR5 Ligands in Rheumatoid Arthritis Synovium. Clin Immunol. 2001;98:39–45.

39. Hanaoka R, Kasama T, Muramatsu M, Yajima N, Shiozawa F, Miwa Y, et al. A novel mechanism for the regulation of IFN-γ inducible protein-10 expression in rheumatoid arthritis. Arthritis Res Ther. 2003;5:R74.
40. Pandya JM, Lundell A-C, Andersson K, Nordström I, Theander E, Rudin A. Blood chemokine profile in untreated early rheumatoid arthritis: CXCL10 as a disease activity marker. Arthritis Res Ther. 2017;19:20.
41. Wang H, Wang T, Dai L, Cao W, Ye L, Gao L, et al. Effects of CXCL3 on migration, invasion, proliferation and tube formation of trophoblast cells. Placenta Netherlands. 2018;66:47–56.
42. Xin H, Cao Y, Shao M-L, Zhang W, Zhang C-B, Wang J-T, et al. Chemokine CXCL3 mediates prostate cancer cells proliferation, migration and gene expression changes in an autocrine/paracrine fashion. Int Urol Nephrol Netherlands. 2018;50:861–8.
43. Zhao Q-Q, Jiang C, Gao Q, Zhang Y-Y, Wang G, Chen X-P, et al. Gene expression and methylation profiles identified CXCL3 and CXCL8 as key genes for diagnosis and prognosis of colon adenocarcinoma. J Cell Physiol United States. 2020;235:4902–12.
44. Li J, Tang Z, Wang H, Wu W, Zhou F, Ke H, et al. CXCL6 promotes non-small cell lung cancer cell survival and metastasis via down-regulation of miR-515-5p. Biomed Pharmacother Biomedecine Pharmacother France. 2018;97:1182–8.
45. Liu G, An L, Zhang H, Du P, Sheng Y. Activation of CXCL6/CXCR1/2 Axis Promotes the Growth and Metastasis of Osteosarcoma Cells in vitro and in vivo. Front Pharmacol. 2019;10:307.
46. Zheng S, Shen T, Liu Q, Liu T, Tuerxun A, Zhang Q, et al. CXCL6 fuels the growth and metastases of esophageal squamous cell carcinoma cells both in vitro and in vivo through upregulation of PD-L1 via activation of STAT3 pathway. J Cell Physiol. United States; 2020.
47. Pokorny V. Evidence for negative association of the chemokine receptor CCR5 d32 polymorphism with rheumatoid arthritis. Ann Rheum Dis. 2004;64:487–90.
48. van Kuijk AWR, Vergunst CE, Gerlag DM, Bresnihan B, Gomez-Reino JJ, Rouzier R, et al. CCR5 blockade in rheumatoid arthritis: a randomised, double-blind, placebo-controlled clinical trial. Ann Rheum Dis. 2010;69:2013–6.
49. Takeuchi T, Kameda H. What is the future of CCR5 antagonists in rheumatoid arthritis? Arthritis Res Ther. 2012;14:114.
50. Lan Y, Wang Y, Liu Y. CCR5 silencing reduces inflammatory response, inhibits viability, and promotes apoptosis of synovial cells in rat models of rheumatoid arthritis through the MAPK signaling pathway. J Cell Physiol. 2019;234:18748–62.
51. Quinones MP, Estrada CA, Kalkonde Y, Ahuja SK, Kuziel WA, Mack M, et al. The complex role of the chemokine receptor CCR2 in collagen-induced arthritis: implications for therapeutic targeting of CCR2 in rheumatoid arthritis. J Mol Med. 2005;83:672–81.
52. Pedraza-Arévalo S, Hormaechea-Agulla D, Gómez-Gómez E, Requena MJ, Selth LA, Gahete MD, et al. Somatostatin receptor subtype 1 as a potential diagnostic marker and therapeutic target in prostate cancer. Prostate. 2017;77:1499–511.

53. Zhao J, Liang Q, Yu J. Somatostatin Receptor 1, a novel EBV-associated CpG hypermethylated gene, contributes to the pathogenesis of EBV-associated gastric cancer. Br J CANCER. 2013;8.

Tables

Table 1 The GO functional enrichment analysis

Category	Term	Count	P. value
BP	signal transduction	77	1.52×10^{-08}
	immune response	62	1.94×10^{-22}
	G-protein coupled receptor signaling pathway	55	2.58×10^{-05}
	inflammatory response	43	1.11×10^{-11}
	cell adhesion	42	1.31×10^{-08}
MF	calcium ion binding	36	8.61×10^{-03}
	protein homodimerization activity	34	2.89×10^{-02}
	protein heterodimerization activity	31	2.16×10^{-04}
	receptor binding	27	7.03×10^{-05}
	chemokine activity	19	4.15×10^{-15}
CC	plasma membrane	233	2.26×10^{-20}
	integral component of membrane	223	7.79×10^{-07}
	extracellular region	116	3.43×10^{-16}
	integral component of plasma membrane	110	8.23×10^{-18}
	extracellular space	82	5.37×10^{-08}

Table 2 The KEGG pathway analysis

Term	Count	P. value
Cytokine-cytokine receptor interaction	48	$6.86\ 10^{-21}$
Chemokine signaling pathway	31	2.03×10^{-11}
Neuroactive ligand-receptor interaction	26	7.30×10^{-05}
Cell adhesion molecules (CAMs)	24	4.71×10^{-09}
Systemic lupus erythematosus	20	9.23×10^{-07}
T cell receptor signaling pathway	16	6.59×10^{-06}
Hematopoietic cell lineage	15	5.80×10^{-06}
Rheumatoid arthritis	14	3.24×10^{-05}
Transcriptional misregulation in cancer	14	1.35×10^{-02}
Primary immunodeficiency	13	2.55×10^{-09}
Natural killer cell mediated cytotoxicity	12	7.98×10^{-03}
Intestinal immune network for IgA production	11	1.02×10^{-05}
Leukocyte transendothelial migration	10	3.56×10^{-02}
Autoimmune thyroid disease	9	8.30×10^{-04}
Viral myocarditis	9	1.54×10^{-03}

Table 3 The gene primer sequence

Gene	Primer Sequence
SSTR3	FORWARD 5’-ATGGACATGCTTCATCCATCAT-3’
	REVERSE 5’-CACATAGATGACCAGCGAGTTA-3’
SSTR1	FORWARD 5’-TGTTGTACACATTTCTCATGGG-3’
	REVERSE 5’-CATCTTAGCAATGATGAGCACG-3’
CCR5	FORWARD 5’-GCAGCTCTCATTTTCCATACAG-3’
	REVERSE 5’- GACACCGAAGCAGAGTTTTTAG-3’
CCR7	FORWARD 5’-CATGCTCCTACTTCTTTGCATC-3’
	REVERSE 5’-CACTGTGGCTAGTATCCAGATG-3’
CXCL6	FORWARD 5’-TGAGAGTAAACCCCAAAACGAT-3’
	REVERSE 5’-CAAACTTGCTTCCCGTTCTTC-3’
CXCL3	FORWARD 5’-GCGTCCGTGGTCACTGAACTG-3’
	REVERSE 5’-AGTGTGGCTATGACTTCGGTTTGG-3’
CCR2	FORWARD 5’-CCAACGAGAGCGGTGAAGAAGTC-3’
	REVERSE 5’- CGAGTAGAGCGGAGGCAGGAG-3’
CXCR5	FORWARD 5’-CGGCAGACACGCAGTTCCAC-3’
	REVERSE 5’-ACGGCAAAGGGCAAGATGAAGAC-3’
CXCL10	FORWARD 5’-CTCTCTCTAGAACTGTACGCTG-3’
	REVERSE 5’-ATTCAGACATCTCTTCTCACCC-3’
CXCL13	FORWARD 5’-CAAGGTGTTCTGGAGGTCTATT-3’
	REVERSE 5’-TGAATTCGATCAATGAAGCGTC-3’

Figures

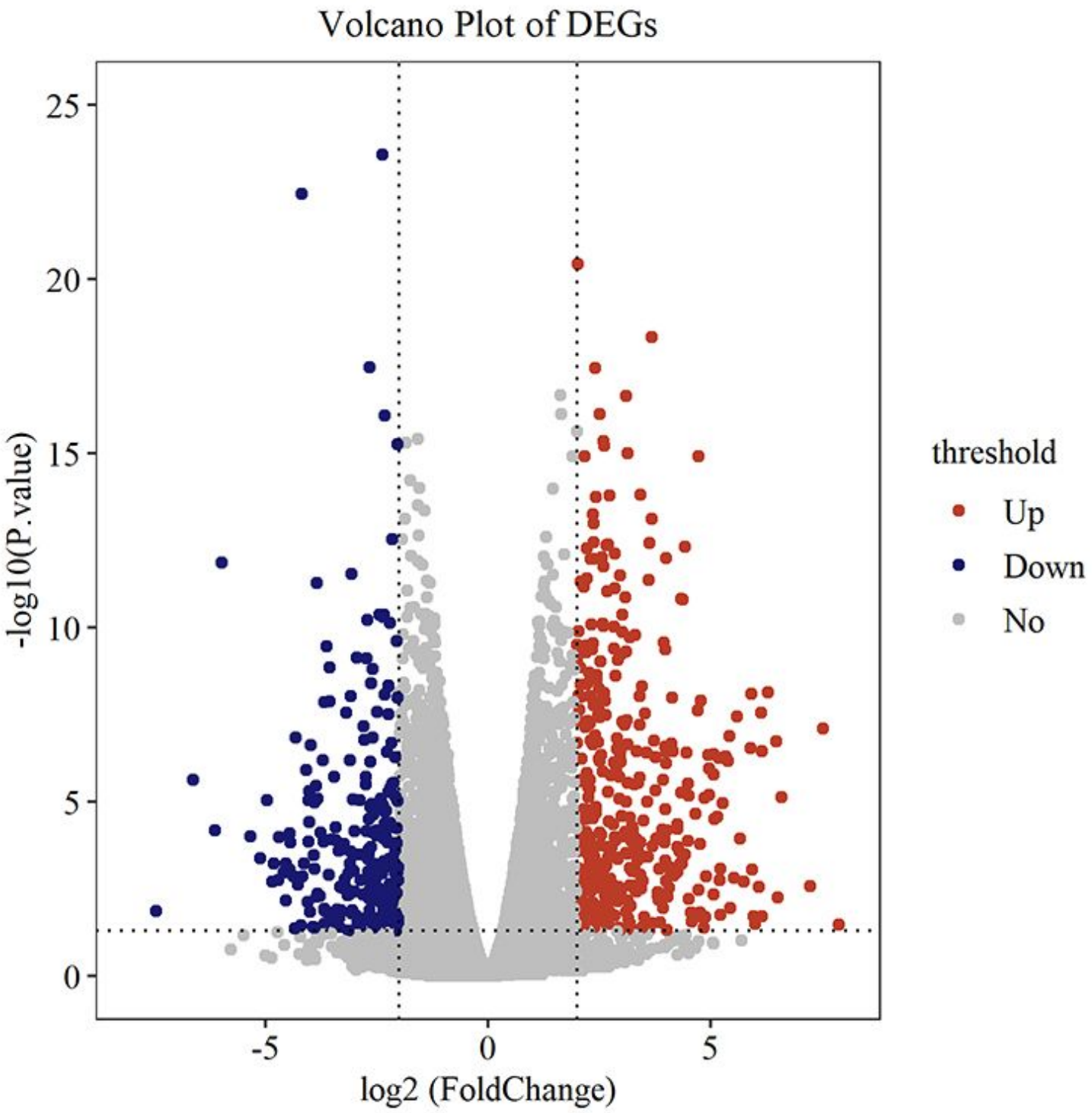

Figure 1

The Volcano Plot of DEGs. The red dots represent up-regulated genes and the blue dots represent down-regulated genes

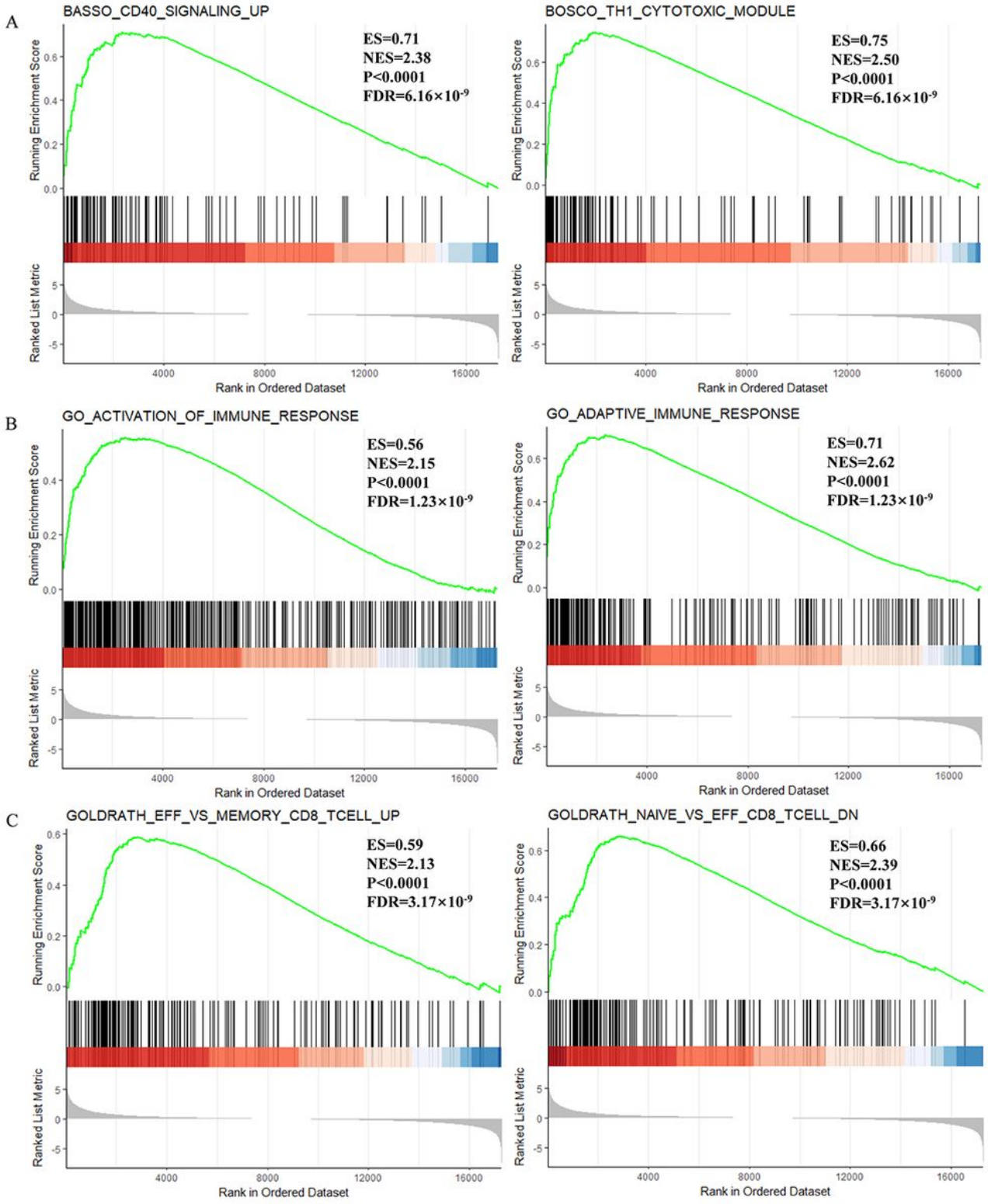

Figure 2

GSEA plot of total detected genes. A:C3 (curated gene sets); B: C5 (ontology gene sets); C: C7 (immunologic signature gene sets). GSEA: Gene set enrichment analysis; ES: enrichment score; NES: normalized enrichment score.

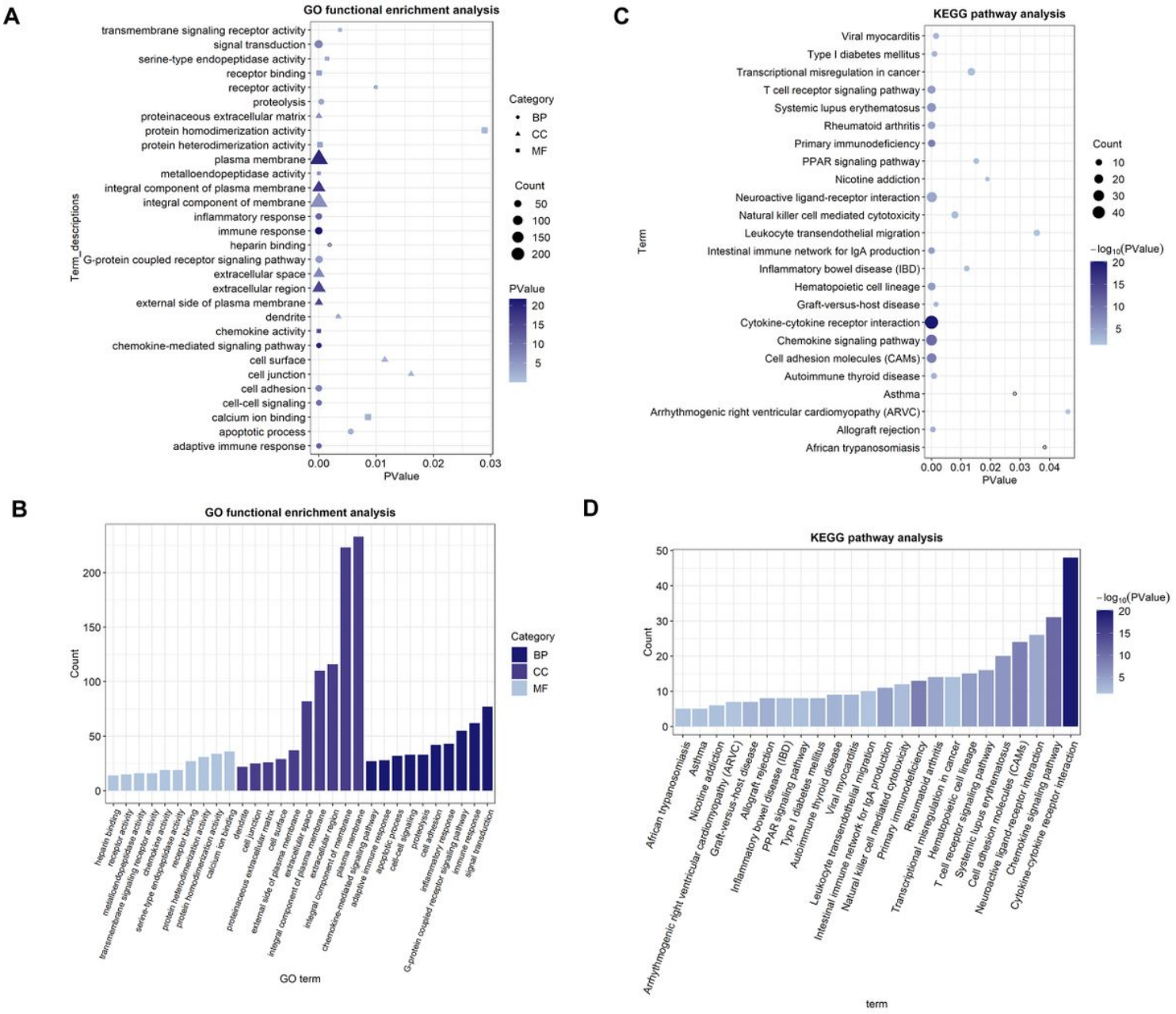

Figure 3

GO functional enrichment and KEGG pathway analysis of DEGs. A: the dot plot of GO functional enrichment analysis (the top 5 terms of each category); B the bar plot of GO functional enrichment analysis (the top 5 terms of each category); C the dot plot of KEGG pathway analysis; D the bar plot of KEGG pathway analysis.

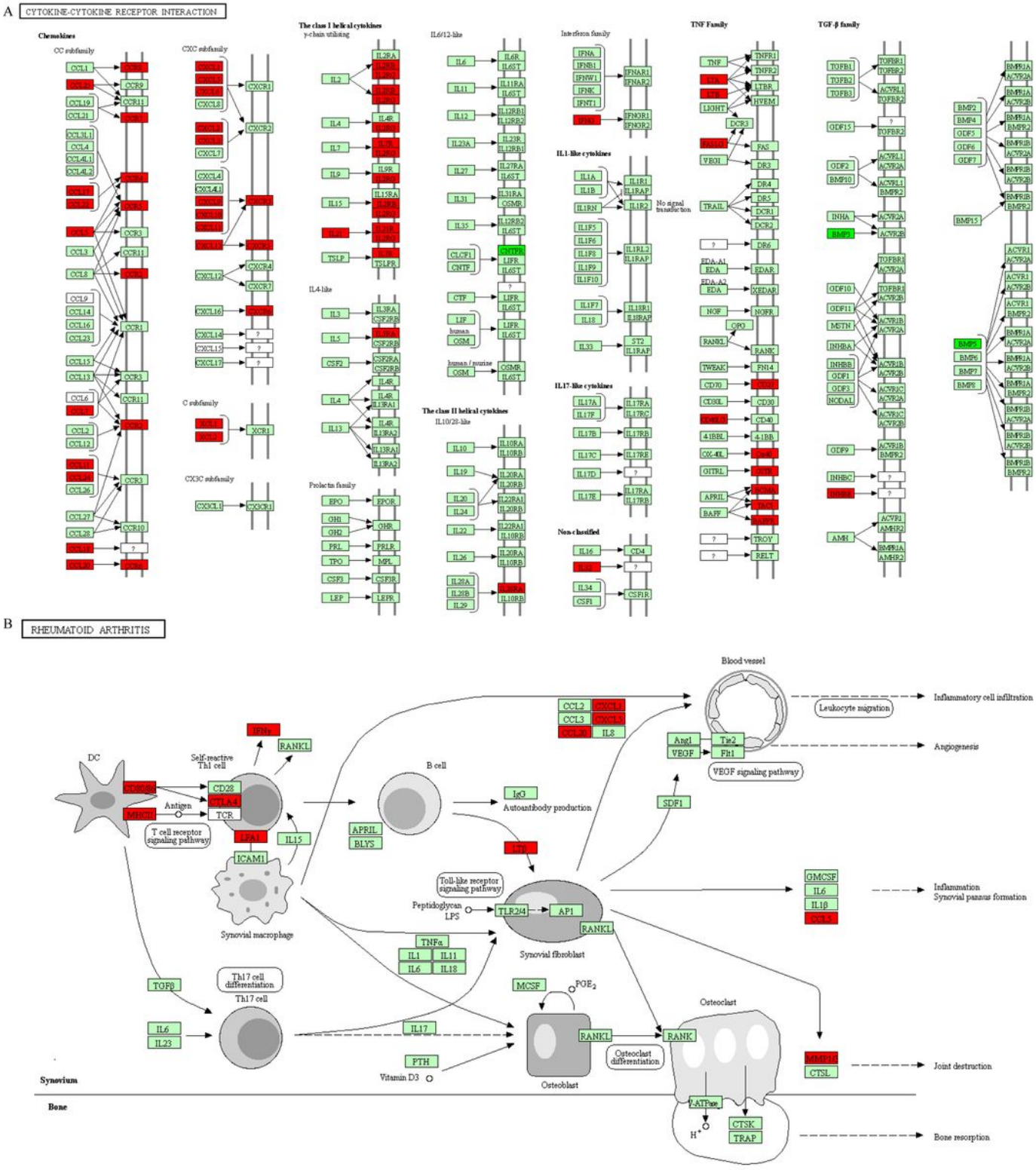

Figure 4

Two important pathways in KEGG pathway analysis. A: The cytokine-cytokine receptor interaction pathway; B: The rheumatoid arthritis pathway. The red boxes represent up-regulated genes and the dark green boxes represent down-regulated genes.

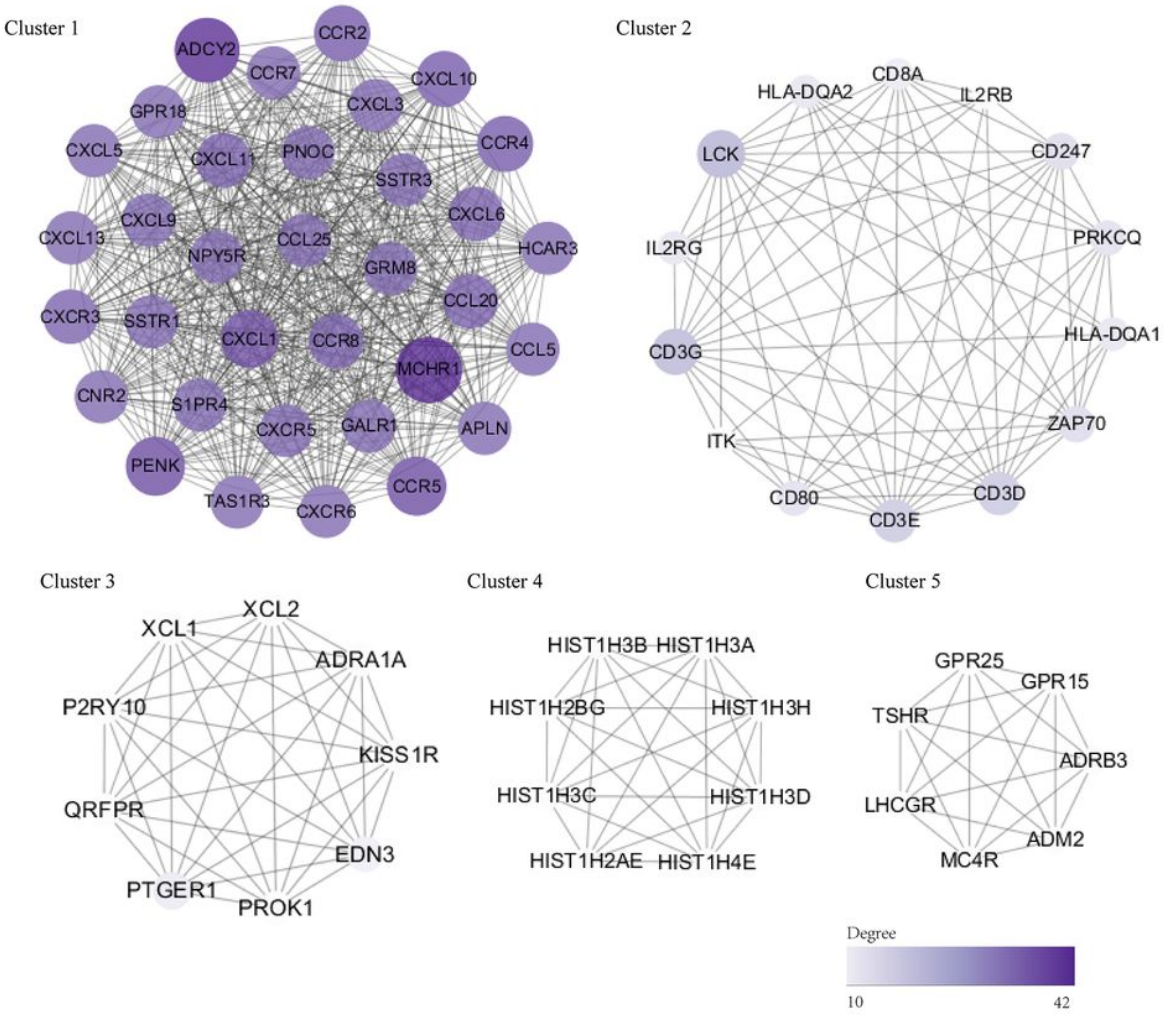

Figure 5

The PPI network construction and hub genes identification (top 5 modules). The significant modules identified by MCODE plugin of Cytoscape. The size and color of the circle represent the degree of the hub gene. The darker the color, the bigger the circle, the greater the degree of the core gene. DEG: differentially expressed gene; PPI: protein–protein interaction.

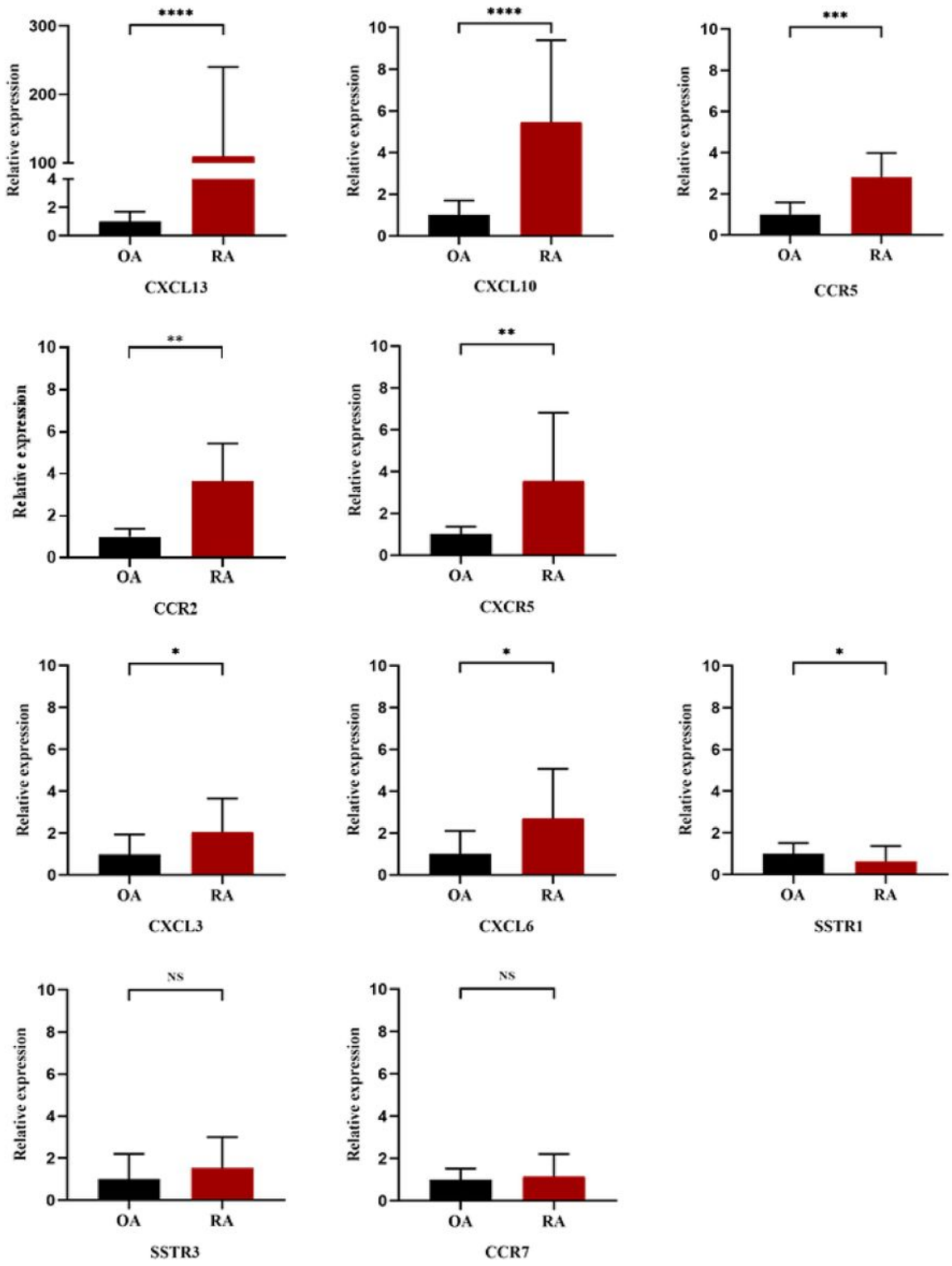

Figure 6

Validation of the 10 hub genes by qRT-PCR between the RA and OA synovial tissue. The relative expression levels of each gene were calculated using 2−ΔΔCt methods. ∗∗∗∗ represents P< 0.0001, ∗∗∗ represents P< 0.005, ∗∗ represents P< 0.01, ∗ represents P< 0.05.

Supplementary Files

This is a list of supplementary files associated with this preprint. Click to download.

- SupplementaryTable1.docx